between M81 and M82. The velocity of M82 matches the velocity perturbation associated with HVT both in sign and magnitude. The disk orbital period at 15-kpc radius is 5×10^8 yr, and the extent of the HVT suggests that M82 passed through the western disk of M81 near $R \approx 15$ kpc some 2×10^8 yr ago. In this scenario, the Magellanic-type dwarf Ho IX found 10 arcmin east of M81, concentration I, and the $10^6 M_\odot$ molecular complex found near the H I peak[25], can be explained as the resultant stellar and gaseous debri.

Arp ring and concentration II. The main body of the Arp ring[26], a faint halo-like optical structure found just north of M81, in fact coincides with the outer H I arm of M81. Concentration II is the brightest H I complex in the tidal bridge between M81 and M82 (Fig. 1), and it coincides with the brightest optical segment of the Arp ring. The high H I column density in this direction is due to the fact that this is the site where the tidally stripped gas from M81, the tidal streamer from M82, and the north tidal bridge intersect, each with distinct velocities and velocity widths. The Arp ring may not be a single cohesive feature.

NGC3077 and tidal bridges. The north and south tidal bridges could be interpreted as a single continuous 100-kpc-long tidal feature, which connects smoothly to one of the tidally induced spiral arms of M81. We find a local H I peak near the stellar nucleus of NGC3077 while the bulk of the $7 \times 10^8 M_\odot$ H I complex is displaced by ~4 kpc from the stellar peak. The H I velocity gradient across the major axis of NGC3077 is consistent with rotation. The isovelocity contours along the south tidal bridge are perpendicular to its length as expected for a tidal tail (for example, NGC7252; ref. 27), but those along the north tidal bridge, particularly near NGC3077, are along the length, as might be expected for tidally induced shearing motion, similar to that of the remnant disk around M82. This suggests that NGC3077, now appearing as a gas-poor dwarf elliptical[28–30], could have been the origin for the gas complex around NGC3077 and the north tidal bridge.

M82. Earlier low-resolution studies by Cottrell[11] and others had interpreted the north–south overall velocity gradient perpendicular to the stellar disk as that of a tidally captured H I cloud in a polar orbit. Our recent high-resolution H I study of M82 using the VLA[17] found luminous H I streamers 10–20 kpc long emerging from the warped stellar disk, and both the two-arm morphology and the smooth connection of their velocity fields onto the disk rotation are cited as the evidence for the tidal disruption of the outer H I disk of M82 by a massive companion (M81) in a polar orbit. Our study strengthens these conclusions by tracing previously discovered H I tails to greater and fainter extents (>30 kpc). The original H I disk of M82 was probably quite substantial before the tidal disruption by M81.

The synthesis of a large mosaic in H I with good angular resolution, as has been done here, can demonstrate the effect of tidal interactions on the evolution of galaxies in small groups, especially when there is little sign of close interactions in optical images. The observations presented here suggest that the presence of even a minor companion may drastically increase the apparent gaseous extent of galaxies. Further sensitive studies of other groups of galaxies will show whether the optical or H I appearances of galaxies are better indicators of the nature and history of the system. □

Received 19 July; accepted 9 November 1994.

1. Sanders, D. B. *et al. Astrophys. J.* **325,** 74–91 (1988).
2. Scoville, N. Z. & Soifer, B. T. *Massive Stars and Starburst* (ed. K. Leitherer) 233–252 (Cambridge Univ. Press, 1991).
3. Barnes, J. E. *Astrophys. J.* **331,** 669–717 (1988).
4. Barnes, J. E. & Hernquist, L. E. *Astrophys. J.* **370,** L65–L69 (1991).
5. Freedman, W. L. *et al. Astrophys. J.* **427,** 628–655 (1994).
6. Visser, H. C. D. *Structure and Properties of Nearby Galaxies* (eds Berkhuijsen E. M. & Wielebinski, R.) 105–112 (Reidel, Dordrecht, 1978).
7. Peimbert, N. & Torres-Peimbert, S. *Astrophys. J.* **245,** 845–856 (1981).
8. Wisniewski, W. Z. & Kleinmann, D. E. *Astr. J.* **73,** 866–867 (1968).
9. Rieke, G. H., Lebofsky, M. J., Thompson, R. I., Low, F. J. & Tokunaga, A. T. *Astrophys. J.* **238,** 24–40 (1980).
10. Roberts, M. S. *External Galaxies and Quasi Stellar Objects* (ed. Evans, D. S.) 12–36 (Reidel, Dordrecht, 1972).
11. Cottrell, G. A. *Mon. Not. R. astr. Soc.* **178,** 577–589 (1977).
12. Gottesman, S. T. & Weliachew, L. *Astrophys. J.* **211,** 47–61 (1977).
13. van der Hulst, J. M. *Astr. Astrophys.* **75,** 97–111 (1979).
14. Rots, A. H. *Astr. Astrophys. Suppl. Ser.* **41,** 189–209 (1980).
15. Appleton, P. N., Davies, R. D. & Stephenson, R. J. *Mon. Not. R. astr. Soc.* **195,** 327–352 (1981).
16. Cottrell, G. A. *Mon. Not. R. astr. Soc.* **174,** 455–466 (1976).
17. Yun, M. S., Ho, P. T. P. & Lo, K. Y. *Astrophys. J.* **411,** L17–L20 (1993).
18. Kent, S. M. *Astr. J.* **93,** 816–832 (1987).
19. Gottesman, S. T. & Weliachew, L. *Astrophys. J.* **195,** 23–45 (1975).
20. Lin, C. C., Yuan, C. & Shu, F. H. *Astrophys. J.* **155,** 721–746 (1969).
21. Rots, A. H. *Astr. Astrophys.* **45,** 43–55 (1975).
22. Toomre, A. & Toomre, J. *Astrophys. J.* **178,** 623–666 (1972).
23. Rots, A. H. & Shane, W. W. *Astr. Astrophys.* **45,** 25–42 (1975).
24. Appleton, P. N. & van der Hulst, J. M. *Mon. Not. R. astr. Soc.* **234,** 957–969 (1988).
25. Brouillet, N., Henkel, C. & Baudry, A. *Astr. Astrophys.* **262,** L5–L8 (1992).
26. Arp, H. *Science* **148,** 363–364 (1965).
27. Hibbard, J. E., Guhathakurta, P., van Gorkom, J. H. & Schweizer, F. *Astr. J.* **107,** 67–89 (1994).
28. Demoulin, M. *Astrophys. J.* **157,** 81–85 (1960).
29. Barbieri, C., Bertola, F. & di Tullio, G. *Astr. Astrophys.* **35,** 463–466 (1974).
30. Price, J. S. & Gullixson, C. A. *Astrophys. J.* **337,** 658–670 (1989).

ACKNOWLEDGEMENTS. NRAO and VLA are operated by Associated Universities, Inc., under cooperative agreement with the US National Science Foundation.

Superconductivity in a layered perovskite without copper

Y. Maeno*, H. Hashimoto*, K. Yoshida*, S. Nishizaki*, T. Fujita*, J. G. Bednorz† & F. Lichtenberg†‡

* Department of Physics, Hiroshima University, Higashi-Hiroshima 724, Japan
† IBM Research Division, Zürich Research Laboratory, 8803 Rüschlikon, Switzerland

FOLLOWING the discovery of superconductivity at ~30 K in $La_{2-x}Ba_xCuO_4$ (ref. 1), a large number of related compounds have been found that are superconducting at relatively high temperatures. The feature common to all of these materials is a layered crystal structure based on a perovskite template and containing planar networks of copper and oxygen. This raises the question of whether superconductivity can occur in layered perovskites that do not contain copper. To the best of our knowledge, no such material has been found to date, despite nearly a decade of searching. We describe here the discovery of superconductivity in Sr_2RuO_4, a layered perovskite isostructural with $La_{2-x}Ba_xCuO_4$ (Fig. 1). Our results demonstrate that the presence of copper is not a prerequisite for the existence of superconductivity in a layered perovskite. But the low value of the superconducting transition temperature (T_c = 0.93 K) points towards a special role for copper in the high-temperature superconductors.

The compound Sr_2RuO_4 has been known for quite some time[2]. It is the $n = 1$ member of the homologous series expressed as $Sr_{n+1}Ru_nO_{3n+1}$, of which those members with $n = 1, 2$ and ∞ have been synthesized[2,3]. Single crystals of Sr_2RuO_4 used in the present study were grown in air by a floating-zone method[4]. They are easily cleaved, yielding plate-like crystals with (001) surfaces. Electron-probe microanalysis indicated a homogeneous distribution of the metal ions within a crystal and did not detect any impurity inclusions. All the observed peaks of powder X-ray diffraction spectra on crushed crystals are consistent with a body-centred tetragonal unit cell of the K_2NiF_4 structure with lattice parameters $a = b = 0.387$ nm and $c = 1.274$ nm at room temperature, in good agreement with the previous reports[2,4].

The low-temperature measurements were performed by using ^{3}He refrigerator (Heliox, made by Oxford Instruments, Eynsham, UK). Figure 2 shows the alternating current (a.c.) suscept-

‡ Present address: VARTA Betterie AG, R and D Centre, 65779 Kelkheim, Germany.

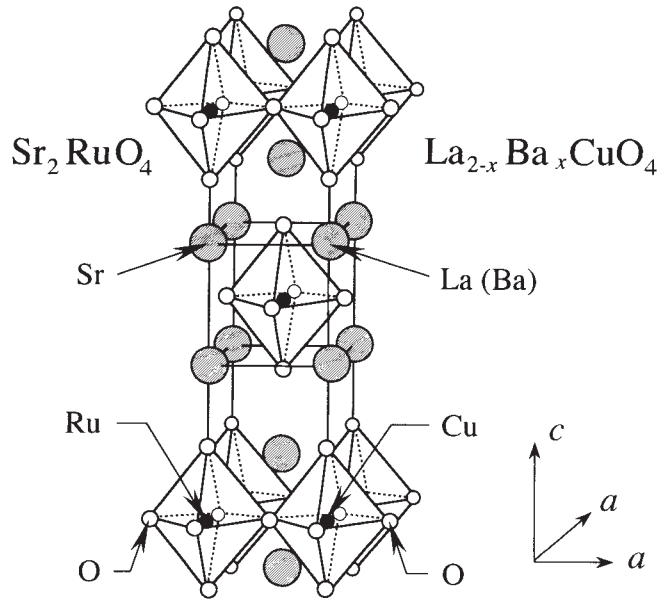

FIG. 1 Schematic crystal structure of superconductors Sr_2RuO_4 and $La_{2-x}Ba_xCuO_4$. Also shown are the directions of the tetragonal principal axes. ($b = a$ in a tetragonal structure.)

ibility of a crystal with the dimensions 3 mm^2 × 0.2 mm under a magnetic field parallel to the c-axis. A strong diamagnetic signal (χ') associated with the Meissner effect was observed below 1 K. Although it did not reach a saturated value even at 0.32 K, the magnitude of χ' is already comparable to that obtained for a high-quality single crystal of $La_{2-x}Sr_xCuO_4$ ($x = 0.15$) with similar volume and shape. Also shown is the dissipative component χ'', which exhibits characteristic peaks below T_c.

Figure 3 gives the electrical resistivity below 4 K with the current both parallel (ρ_{ab}) and perpendicular (ρ_c) to the RuO_2 plane, showing the superconducting transition at T_c slightly below 1 K. The sizes of the crystals were typically (1–2) × 2 × 0.1 mm^3. Within our experimental precision of ~10 nV for the voltage detection, zero resistivity was achieved in both ρ_{ab} and ρ_c at low temperatures. The critical-current densities were measured at 0.32 K. By increasing the measurement current, normal-state resistivity abruptly recovered beyond $j_c = 2.0$ and 0.018 A cm^{-2}, respectively within the ab-plane and along the c-axis. These values give the anisotropy ratio of 110. The resistivity curves in Fig. 3 were taken at the current densities which are half of the respective j_cs at 0.32 K. From the midpoint of the resistive transition, as well as from the diamagnetic onset, $T_c = 0.93 \pm 0.03$ K for all the as-grown crystals we have examined.

Figure 4 displays the anisotropy in the normal-state resistivity. The resistivity ratios are $\rho_c/\rho_{ab} = 220$ at 290 K and 850 at 2 K. The most striking feature is the crossover in ρ_c from non-metallic to metallic behaviour with a broad maximum at $T_M \approx 130$ K, as reported previously[4]. However, improved measurements in the present study clarify subtle but important details: a change in the temperature dependence of ρ_{ab} at the corresponding temperature also becomes evident. At high temperatures, the conduction is metallic only within the plane as in $La_{2-x}Sr_xCuO_4$ with light and

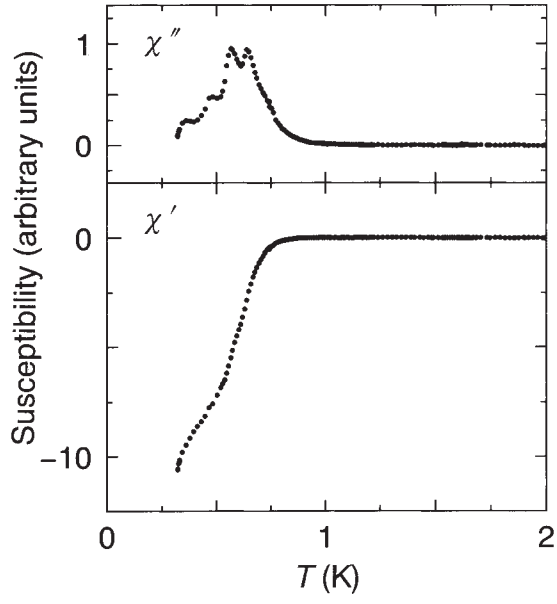

FIG. 2 The a.c. susceptibility of a single crystal of Sr_2RuO_4 measured by a mutual-inductance method at a magnetic field of $H = 0.67$ Oe (root-mean-squares value) parallel to the c-axis, and at a frequency of 1,000 Hz. Top, χ'' (imaginary part); bottom, χ' (real part).

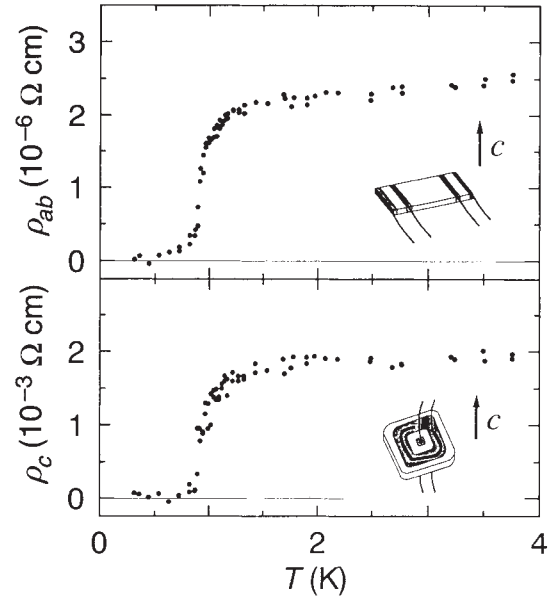

FIG. 3 Anisotropy in the resistivity ρ of Sr_2RuO_4 below 4 K. The superconducting transition is at $T_c = 0.93$ K. Insets, attachment of the electrodes.

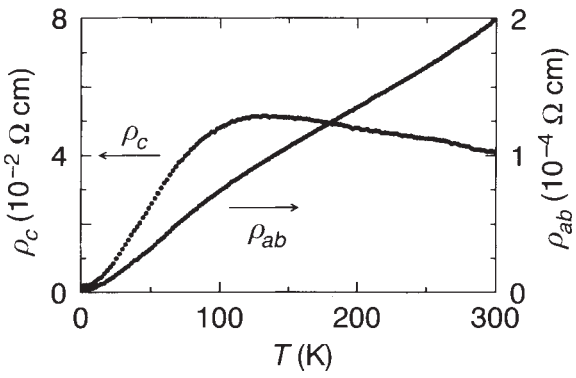

FIG. 4 Anisotropy in the resistivity of Sr_2RuO_4 below 300 K.

optimal doping; at low temperatures, the conduction becomes metallic in all three directions as in $La_{2-x}Sr_xCuO_4$ with heavy doping[5].

We further investigated the normal-state properties mainly by using sintered polycrystalline samples. The magnetic susceptibility is characterized by an enhanced temperature-independent component, $\chi_0 = 9.7 \times 10^{-4}$ e.m.u. mol^{-1}. The Sommerfeld coefficient, or the temperature-linear coefficient in the specific heat is $\gamma = 39$ mJ K^{-2} mol^{-1}. Both of these values are enhanced several times from those of RuO_2 (refs 6, 7), which is considered as an ordinary *d*-band metal[8], and are even greater than those observed in $Sr_{1-x}La_xTiO_3$ on the verge of metal/Mott-insulator transition[9]. For another comparison, $\gamma = 10$–15 mJ K^{-2} mol^{-1} for optimally doped $La_{2-x}Sr_xCuO_4$ (M. Ido, personal communication). Moreover, the Wilson ratio[10] of Sr_2RuO_4, $R_W = (\pi^2 k_B^2/3\mu_B^2)(\chi_0/\gamma) = 1.8$ (where k_B is the Boltzmann constant, μ_B is the Bohr magneton and γ is expressed in erg K^{-2} mol^{-1}), indicates that the enhancement in both χ_0 and γ are of the same origin. Although the resistivity of the polycrystalline samples were three orders of magnitude greater than ρ_{ab}, probably due to poor conductivity of the grain boundaries, it did show a strong reduction below 2.3 K and it became as small as 25% of the onset superconducting value when the sample was cooled to 50 mK in a dilution refrigerator. Nevertheless, zero resistivity was never attained in our sintered samples. The magnetic susceptibility of a sintered sample also exhibited a diamagnetic transition at ~1 K. The details of these results will be reported elsewhere. The origin of the discrepancies in T_c between the single crystals and the sintered samples is not understood at present.

The electronic structure of Sr_2RuO_4 has a number of similarities to that of copper oxide superconductors, although the 3*d* electrons of Cu are replaced by the 4*d* electrons of Ru. As suggested by photoelectron spectroscopy[11] of related compounds, the states near the Fermi level are composed of hybridized Ru-4*d* and O-2*p* states. The presence of strong Coulomb correlations among the electrons is reflected in their enhanced effective mass, as well as by the fact they $Y_2Ru_2O_7$ with a distorted array of corner-shared RuO_6 octahedra[12] is non-metallic because of correlation-induced electron localization[11].

It is well known[13] that ρ_c of $La_{2-x}Sr_xCuO_4$ is profoundly affected by the structural transition from the high-temperature tetragonal phase to the mid-temperature orthorhombic phase. We investigated the low-temperature structure of Sr_2RuO_4 by powder X-ray diffraction of crushed crystals, but did not detect any structural transition down to 5 K or any change in the temperature dependence of the lattice parameters across T_M. This result is consistent with a previous structure refinement[14] at 100 K. Therefore the origin of the sign change in $d\rho_c/dT$ with temperature in the present system appears to be purely electronic, although we still need to clarify whether a subtle (or local) change in the structure exists. The resistivity behaviour may be explained in terms of the criterion for three-dimensional anisotropic metals as was done for copper oxide superconductors[5], or alternatively in terms of a competition between the transfer energy along the *c*-axis and the thermal energy. In any case, this curious normal-state behaviour alone is worth further investigation.

There are important differences between copper oxide superconductors and Sr_2RuO_4. First, the T_c of isostructural copper oxide superconductors is higher by a factor of 20–40 than that of Sr_2RuO_4. This fact, however, may provide easier comparison between Sr_2RuO_4 and conventional superconductors, because the electronic contribution to various physical quantities near T_c is not overwhelmed by the phonon contribution. Second, the Cu^{2+} ($3d^9$) valence state has spin 1/2, whereas Ru^{4+} ($4d^4$) is in the low-spin state with spin 1, as demonstrated[15] in $Sr_2Ir_{1-x}Ru_xO_4$. The important *d*–*p* hybridization occurs with $e_g(d_{x^2-y^2})$ orbitals in the copper oxides, in contrast to t_{2g} orbitals in Sr_2RuO_4. Many of the existing theories for copper oxide superconductors rely upon peculiar normal states derived from the spin-1/2 state. (see, for example, ref. 16). Intriguingly, when we measured the resistivity of polycrystalline Sr_2RhO_4, based on Rh^{4+} ($4d^5$) with spin 1/2 we found it to be metallic, with no evidence for superconductivity down to 50 mK. It therefore seems probable that superconductivity in the Ru-based compound involves a different mechanism from that operating in the copper oxides.

Last but not least, superconductivity in the copper oxides is realized only after carrier doping of an insulating parent compound such as La_2CuO_4, whereas Sr_2RuO_4 (without any chemical doping to adjust the carrier concentration) is superconductive by itself. For the copper oxides, new states at the Fermi level are created within the correlation (charge-transfer) gap by carrier doping. In contrast, for the Ru-based oxides similar states are expected[17] to evolve within the correlation (Mott–Hubbard) gap by weakening the effective strength of the electron correlation in order from non-metallic $Y_2Ru_2O_7$ with a highly distorted Ru–O network, to metallic Sr_2RuO_4 with very strong anisotropy, to metallic $CaRuO_3$ with itinerant-electron magnetism[18,19] and to an ordinary *d*-band metal RuO_2. This explains why carrier doping is not necessary in Sr_2RuO_4 and opens a second route to realize superconductivity in layered perovskites. Although this model needs to be substantiated further by detailed spectroscopic measurements, our search for superconductivity in Ru-based oxides has been motivated precisely by this picture. □

Received 16 August; accepted 1 November 1994.

1. Bednorz, J. G. & Müller, K. A. *Z. Phys.* B**64,** 189–193 (1986).
2. Randall, J. J. & Ward, R. *J. Am. chem. Soc.* **81,** 2629–2631 (1959).
3. Williams, T., Lichtenberg, F., Reller, A. & Bednorz, G. *Mater. Res. Bull.* **26,** 763–770 (1991).
4. Lichtenberg, F., Catana, A., Mannhart, J. & Schlom, D. G. *Appl. Phys. Lett.* **60,** 1138–1140 (1992).
5. Ito, T., Takagi, H., Ishibashi, S., Ido, T. & Uchida, S. *Nature* **350,** 596–598 (1991).
6. Fletcher, J. M., Gardner, W. E., Greenfield, B. F., Holdoway, M. J. & Rand, M. H. *J. chem. Soc. A* 653–657 (1968).
7. Passenheim, B. C. & McCollum, D. C. *J. chem. Phys.* **51,** 320–321 (1969).
8. Glassford, K. M. & Chelikowsky, J. R. *Phys. Rev.* B**49,** 7107–7114 (1994).
9. Tokura, Y. *et al. Phys. Rev. Lett.* **70,** 2126–2129 (1993).
10. Yamada, K. *Prog. theor. Phys.* **53,** 970–986 (1975).
11. Cox, P. A., Egdell, R. G., Goodenough, J. B., Hamnett, A. & Naish, C. C. *J. Phys.* C**16,** 6221–6239 (1983).
12. Kanno, R., Takeda, Y., Yamamoto, T., Kawamoto, Y. & Yamamoto, O. *J. Solid St. Chem.* **102,** 106–114 (1993).
13. Kambe, S. *et al. Physica* C**160,** 35–41 (1989).
14. Walz, L. & Lichtenberg, F. *Acta crystallogr.* C**49,** 1268–1270 (1993).
15. Cava, R. J. *et al. Phys. Rev.* B**49,** 11890–11894 (1994).
16. Anderson, P. W. & Zou, Z. *Phys. Rev. Lett.* **60,** 132–135 (1988).
17. Zhang, X. Y., Rozenberg, M. J. & Kotliar, G. *Phys. Rev. Lett.* **70,** 1666–1669 (1993).
18. Bouchard, R. J. & Gillson, J. L. *Mater. Res. Bull.* **7,** 873–878 (1972).
19. Gibb, T. C., Greatrex, R., Greenwood, N. N., Puxley, D. C. & Snowdon, K. G. *J. Solid St. Chem.* **11,** 17–25 (1974).

ACKNOWLEDGEMENTS. We thank our colleagues, especially F. Nakamura, for many useful suggestions and A. Minami for performing EPMA. We also appreciate discussions with K. A. Müller, R. Cava, H. Takagi, K. Yamada and Y. Tokura. Some of the measurements were performed at the Cryogenic Centre of Hiroshima University. This work was supported mainly by a grant from the Electric Technology Research Foundation of Chugoku.